THE JOURNAL OF PHYSICAL CHEMISTRY LETTERS
A JOURNAL OF THE AMERICAN CHEMICAL SOCIETY

pubs.acs.org/JPCL

Letter

Statistical Properties of Bit Strings Sampled from Sycamore Random Quantum Circuits

Sangchul Oh and Sabre Kais*

Cite This: J. Phys. Chem. Lett. 2022, 13, 7469−7475

Read Online

ACCESS | Metrics & More | Article Recommendations | Supporting Information

ABSTRACT: Quantum supremacy has been recently reported for random circuit sampling on the Sycamore processor with 53 qubits. Here, we analyze the statistical properties of bit strings sampled from random quantum circuits. In contrast to classical random bit strings, bit strings sampled from Sycamore random circuits give rise to heat maps with stripe patterns at specific qubits, have more bit 1 than 0, and do not pass the NIST random number tests. The difference between the Sycamore bit strings and classical random bit strings is also demonstrated by the Marchenko−Pastur distribution and the Girko circular law of random matrices. The calculation of Wasserstein distances shows that the Sycamore bit strings are farther from bit strings sampled from Haar-measure random quantum circuits than classical random bit strings. Our results show that random matrices and Wasserstein distances could be used to analyze the performance of quantum computers.

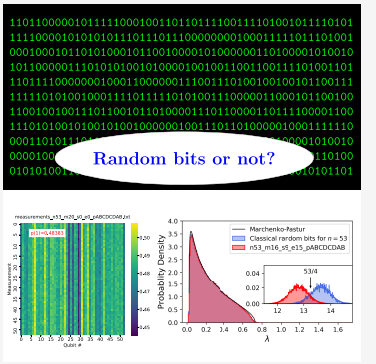

Quantum computers can simulate nature better than classical computers, as noted by Feynman while initiating the idea of quantum computing.[1] Quantum supremacy,[2,3] in which a quantum computer could perform certain computational tasks exponentially faster than a classical computer, is one of the key milestones in developing practical quantum computers. The power of a quantum computer is believed to stem from its quantum nature, such as interference, entanglement, and a large Hilbert space growing exponentially with the number of qubits. The speed-up of quantum algorithms such as Shor's factoring algorithm[4] or the Harrow−Hassidim−Lloyd algorithm for solving linear systems of equations[5] requires a large-scale and error-corrected quantum computer. With the noisy intermediate scale quantum computers currently available, quantum sampling algorithms are considered good candidates to demonstrate quantum supremacy or quantum advantage.[6] There have been recent reports claiming the achievements of quantum supremacy for quantum sampling algorithms on noisy and intermediate-scale quantum computers. In 2019, a Google team[7] claimed the first quantum supremacy by implementing random quantum circuits on 53 superconducting qubits. More recently, Wu et al. performed random quantum circuits with 56 superconducting qubits.[8] In 2020, Zhong et al.[9] reported the quantum advantage in the Gaussian boson sampling with linear optical quantum computers. The aim of the boson sampling task is to sample bit strings from the probability distribution of bosons, given by the permanence of a unitary operator.[10,11]

The quantum supremacy benchmark task of random quantum sampling is to generate bit strings from a particular probability distribution by applying random quantum circuits on qubits followed by the measurement. The probability distribution of bit strings generated by random quantum circuits is not given by a uniform random distribution but obeys the eigenvector distribution of a circular unitary ensemble.[12] The Sycamore quantum processor generated millions of size $n = 53$ bit strings in about 200 s, but a supercomputer with the currently known efficient classical algorithms would take a significantly longer time.[13,14] To verify that a quantum computer implements random quantum circuits correctly, the linear cross-entropy benchmark was introduced.[7,15] The linear cross-entropy benchmark fidelity is calculated with a probability distribution obtained from quantum simulation of random quantum circuits on a classical computer and output bit strings of a quantum computer. Its value was slightly greater than the theoretical threshold, which corresponds to the case of uniformly random bit strings. However, the statistical properties of bit strings obtained from random quantum sampling seem to be unexplored. One may ask whether Sycamore bit strings are as random as classical random bit strings or how far away they are from classical random bit strings or from bit strings sampled from Haar-measure random unitary operators. A rigorous analysis is needed to quantify the performance of random quantum circuits because random unitary dynamics is essential in chaotic scattering,[16−21] quantum information processing,[22]

Received: June 30, 2022
Accepted: August 4, 2022

https://doi.org/10.1021/acs.jpclett.2c02045
J. Phys. Chem. Lett. 2022, 13, 7469−7475

randomized benchmarking of noisy quantum gates,[23−25] scrambling of information in black holes and quantum many-body systems,[26,27] and hydrodynamic simulation[28] in addition to the quantum supremacy benchmark test.

In this Letter, we explore the statistical properties of bit strings sampled from Sycamore random quantum circuits[7,29] using the random matrix theory,[21,30,31] the NIST random number test code,[32] and the Wasserstein distance.[33] To compare with the data set provided by the Sycamore quantum supremacy experiment, classical random bit strings and bit strings sampled from Haar-measure random unitary operators are generated. The heat map patterns of bit strings and the NIST random number tests will show the nonrandomness of Sycamore bit strings and uncover the noise of the Sycamore quantum processor. The difference between Sycamore bit strings and classical random bit strings is illustrated by the positions of outliers of random matrices composed of bit strings. Finally, we will calculate the Wasserstein distance between various data sets of bit strings. It will be shown that Sycamore bit strings are farther from bit strings sampled from Haar-measure unitary operators than classical random bit strings.

Let us start with a brief introduction to the random quantum sampling benchmark and how to verify its faithful implementation. The random quantum circuit benchmark starts with sampling a single random unitary operator $U(2^n)$, then applying it to an input state $|0^n\rangle$ of n qubits and measuring the output state $|\psi\rangle = U|0^n\rangle$ in the computational basis $\{|x\rangle\}$ to generate the bit string $x = a_0a_1\cdots a_{n-1}$ with $a_i \in \{0, 1\}$. The probability of getting a bit string x is given by $p_x \equiv |\langle x|\psi\rangle|^2 = |\langle x|U|0^n\rangle|^2$. By repeating this process M times, an $M \times n$ binary array is obtained.

The first key element of the random quantum sampling is how to draw unitary operators uniformly and randomly, i.e., a random quantum circuit. Mathematically, this could be done with the Haar invariant measure on a $U(2^n)$ unitary group. The collection of these random unitary operators is called a circular unitary ensemble (CUE) introduced by Dyson.[12] The Haar-measure sampling of a unitary operator out of the unitary group is challenging. A unitary operator $U(2^n)$ can be decomposed into the $(2^n - 1)!$ product of two-dimensional unitary transformations, called the Hurwitz decomposition.[34,35] However, this decomposition requires a huge amount of gate operations: the number of 1- or 2-qubit gates is $n^2 \times 2^{2n}$, and the number of parameters is 2^{2n}. Emerson et al.[22] proposed a method of generating pseudorandom unitary operators: the quantum circuit of n random unitary rotations on single qubits with $3n$ parameters followed by the simultaneous two-body interactions on n qubits are repeated m times. On a classical computer, random unitary matrices can be generated by the QR decomposition of matrices with Gaussian random complex elements.[36] The QR algorithm needs $O((2^n)^3)$ floating point operations.

The second key element of the random quantum sampling is the statistical property of the probability p_x finding a qubit state $|\psi\rangle = U|0\rangle$ in $|x\rangle$. A qubit state evolved by a random unitary operator distributes uniformly in a 2^n dimensional Hilbert space. The amplitudes c_x of $|\psi\rangle = \sum_x c_x|x\rangle$ may have the Gaussian distribution on the surface of a 2×2^n dimensional sphere. This leads to the probability distribution $P(p)$ for the random variable p (dropping the subscript x of p_x)

$$P(p) = (N - 1)(1 - p)^{N-2} \tag{1}$$

This is the chi-square distribution with 2 degrees of freedom $\chi_2^2(p)$. It is also known as the eigenvector distribution of a circular unitary ensemble.[16,17,20,21] For large N, it becomes $P(p) = Ne^{-Np}/(1 - e^{-N}) \approx Ne^{-Np} = \chi_2^2(p)$. The expectation value of finding p with respect to $P(p)$ is given by $1/N$. This is consistent with our intuition that classically the probability p_x of finding a bit string x out of N possible bit strings is $1/N$. Note that in some papers[7,15,37] eq 1 is miscalled the Porter−Thomas distribution. However, the Porter−Thomas distribution is given by $P_{PT}(p) = \chi_1^2(p) = \frac{1}{\sqrt{2\pi Np}}e^{-Np/2}$, i.e., the chi-square distribution with 1 degree of freedom and is known as the eigenvector distribution of an Gaussian orthogonal ensemble.[20,21,38,39]

The last key element is to verify the faithful implementation of random quantum circuits. To this end, one has to estimate the empirical probability p_x of finding a random quantum state $|\psi\rangle = U|0\rangle$ in $|x\rangle$ with $x = 0, ..., 2^n - 1$ from the output data, a $M \times n$ binary array. Then one has to construct an empirical probability $P_{em}(p)$ of probabilities p and to compare it to the ideal probability $P(p)$ given by eq 1. For a small number of qubits, the Kullback−Leibler divergence or the cross entropy of $P_{em}(p)$ from $P(p)$ was used to measure how close the probability distribution $P_{em}(p)$ is to the ideal distribution $P(p)$.[15,37]

However, in the quantum supremacy experiment with the Sycamore quantum processor with $n = 53$, the construction of P_{em} was impossible because a few million bit strings are too small to estimate $p(x)$ with $x = 0−9 \times 10^{15}$. Instead, the linear cross-entropy benchmark fidelity $F_{XEB} = 2^n \cdot \frac{1}{M}\sum_{i=1}^{M} p(x_i) - 1$ is introduced.[6,7,37,40,41] Here, x_i are the observed bit strings and the probability $p(x)$ is calculated using the Schrödinger−Feynman simulation of a single random unitary operator for $n = 53$ on a supercomputer.[7,42] In the quantum supremacy experiment,[7] $F_{XEB} = 0.00224$ for $n = 53$ qubits was obtained. A tricky point is that in order to calculate F_{XEB}, i.e., to verify the quantum supremacy for random quantum sampling over a classical computer, one needs the quantum simulation of a random quantum circuit U on a supercomputer. Thus, the verification of random quantum sampling with F_{XEB} may not be scalable.

The measurement data, $M \times n$ bit strings,[29] are the only available information indicating whether the random quantum circuit benchmark was implemented properly on the Sycamore quantum processor. To perform the comparative analysis on the Sycamore bit strings, we generate the two data sets of bit strings. The first data set is classical random bit strings where bits 0 and 1 are equally likely. If bit strings are sampled from the classical uniform random distribution, the cross-entropy benchmark fidelity is known to be $F_{XEB} = 0$. So the classical random bit strings will serve as an indicator to the lower boundary of the performance of random quantum sampling. The second data set is bit strings sampled from a *single* random unitary matrix, an element of a circular unitary ensemble whose distribution is the Haar measure on the unitary group $U(n)$. We call them the CUE bit strings though we deal with a single random unitary operator rather than the ensemble of random unitary operators. It is well known that a random unitary operator can be constructed with the QR decomposition algorithm.[36] A random matrix A with complex elements sampled from the normal distribution is factored as $A = QR$. Then Q is a Haar measure random unitary matrix. The CUE

https://doi.org/10.1021/acs.jpclett.2c02045
J. Phys. Chem. Lett. 2022, 13, 7469−7475

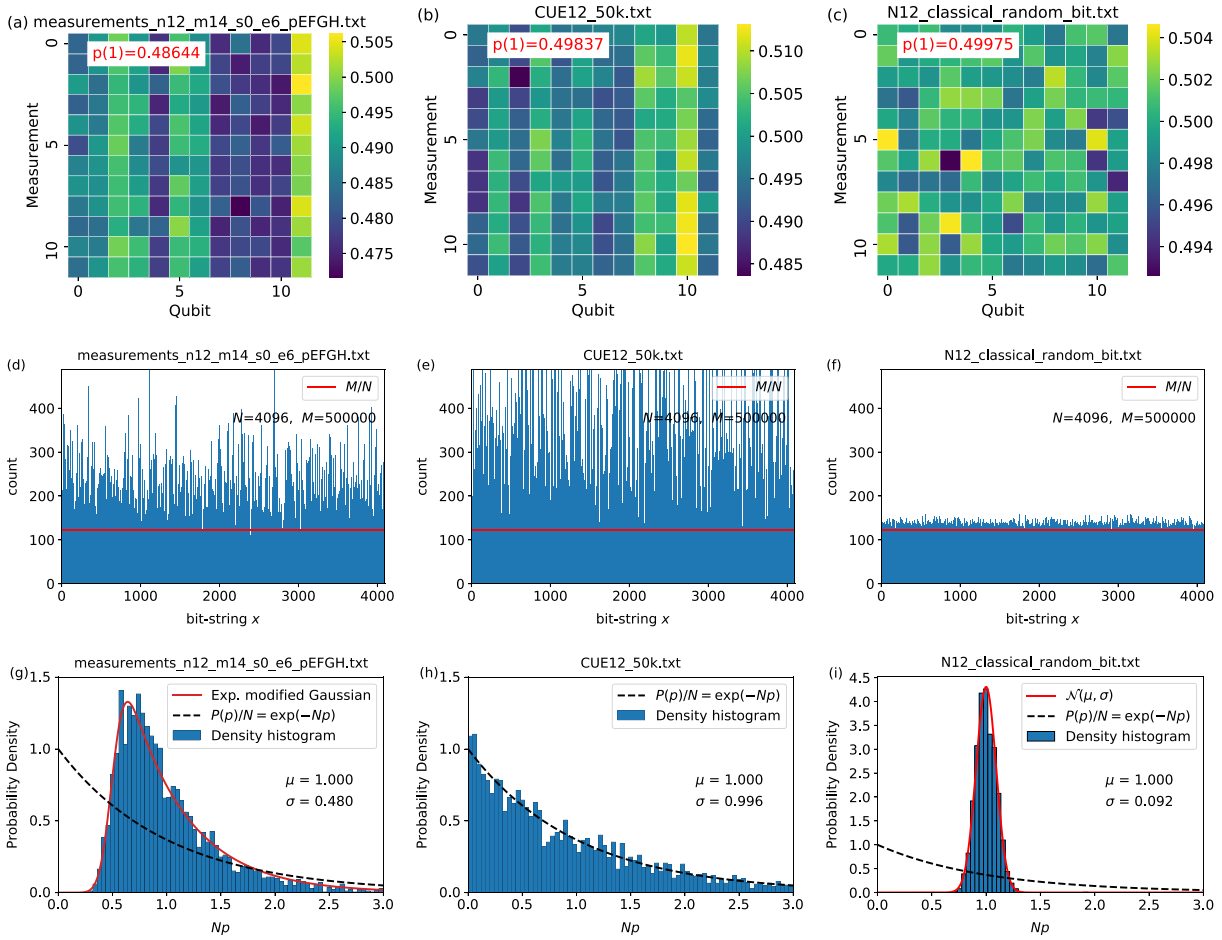

Figure 1. For $n = 12$ and $M = 500\,000$, the first, second, and third columns of figures show bit strings sampled from the Sycamore random circuit,[29] bit strings sampled from a random unitary operator generated with the QR algorithm, and classical random bit strings, respectively. Panels a, b, and c are the heat maps of bit strings. $p(1)$ represents the average of getting bit 1 over all bit strings. Panels d, e, and f are the histograms of bit string x with $0 \le x \le N - 1$. The red lines stand for the average of p_x, $\overline{p} = M/N$. Panels g, h, and i are the empirical probability densities as a function of Np that are constructed from panels d, e, and f. The black lines plot eq 1, $P(p)$. The red lines are fitting curves. The exponentially modified Gaussian distribution has three parameters for location, scale, and shape. The normal distribution is denoted by $\mathcal{N}(\mu, \sigma)$ with the mean μ and the standard deviation σ.

bit string x is sampled from $p_{\mathrm{CUE}}(x) = |\langle x|\psi\rangle|^2 = |\langle x|Q|0\rangle|^2$. The CUE bit strings for $n = 12$ are generated using the Python or Julia random matrix library.[43] The CUE bit strings will be an indicator to the upper limit of the performance of random quantum sampling.

A simple way of testing randomness of bit strings is to detect some underlying patterns. We plot the heat maps of bit strings as shown in Figure 1. By slicing an $M \times n$ rectangular array of bit strings, $D = (x_1, x_2, ..., x_M)^{\mathrm{T}}$, the ensemble of $n \times n$ square binary matrices $\{X_k = (x_{nk+1}, x_{nk+2}, ..., x_{nk+n})^{\mathrm{T}}\}$ is constructed. Here, $x_i = a_1a_2...a_n$ is the ith row of the binary array D and $k = 0, 1, ..., M/n - 1$. Panels a, b, and c of Figure 1 show the heat maps of the average density matrix, $\mathbf{X} = \frac{n}{M}\sum_{k=0}^{M/n} X_k$, with $n = 12$ for the Sycamore bit strings, the CUE bit strings, and the classical random bit strings, respectively. The heat maps for other Sycamore data from $n = 12$ to $n = 53$ and classical random bit strings for $n = 53$ are shown in Figures S1−S3 in the Supporting Information.

Surprisingly, all the heat maps of Sycamore data show the stripe patterns at some qubit indices while the classical random bit strings do not. Some of the CUE bit strings show the stripe patterns, while others do not. As depicted in Figures S1−S3 in the Supporting Information, the two coupler activation types, EFGH and ABCDCDAB, give rise to different bright and dark stripe patterns. For $n = 53$ and ABCDCDAB activation, the stripe patterns become more clear as the cycle number m increases. The total number of bit 1 of binary array D is counted to calculate the average $p(1)$ of finding bit 1. As shown in Figure 1a−c, Sycamore bit strings show the value $p(1) \approx 0.486$, which is less than the expected value of 0.5, while the CUE bit strings and the classical random bit strings have $p(1) \approx 0.498$ and $p(1) \approx 0.50$, which are very close to 0.5. As shown in Figures S1−S3 in the Supporting Information, $p(1)$ for Sycamore bit strings ranges from 0.483 to 0.489. The nonrandomness of Sycamore bit strings can also be checked with a random number test as well as the stripe patterns. We perform the NIST statistical random number tests.[32,44] As shown in Table S1 in the Supporting Information, Sycamore bit strings fail to pass some NIST random number tests while the classical random bit strings pass. The failure of the NIST frequency test indicates that the Sycamore data set has too many 0s.

https://doi.org/10.1021/acs.jpclett.2c02045
J. Phys. Chem. Lett. 2022, 13, 7469−7475

One may speculate that the failure of Sycamore bit strings to pass the NIST random number tests is caused by the measurement error of the Sycamore processor. The Sycamore quantum processor is more likely to produce the measures outcome 0 (the ground state) than outcome 1 (the first excited state).[7] This measurement error possibly accounts for the average of finding bit 1 less than that of finding bit 0 in Sycamore bit strings. However, we find that the Zuchongzhi quantum processor[8] generated data where the average of finding bit 1 is equally likely to that of finding bit 0.[45]

Next, we calculate the empirical distributions $p(x) = b_x/M$ for $n = 12$, where b_x counts the number of bit strings with the value x and $0 \le x \le N - 1$ in decimal notation. As illustrated in Figure 1d–f, Sycamore data show wider fluctuation in the count of bit strings in x than the classical random bit strings but less than the CUE bit strings. Using the empirical distribution $p(x)$, we construct the three empirical probability distributions $P_{\text{Sycamore}}(p)$, $P_{\text{CUE}}(p)$, and $P_{\text{cl}}(p)$ to see if they follow eq 1, the eigenvector distribution of the circular unitary ensemble. As shown in Figure 1g–i, the probability $P_{\text{CUE}}(p)$ for the CUE bit strings follows eq 1, $P(p)/N = \exp(-Np)$, but $P_{\text{Sycamore}}(p)$ for the Sycamore bit strings deviates from it. As expected, $P(p)$ for the classical random bit strings is given by the Gaussian distribution. This analysis implies that the quantum supremacy benchmark test for random quantum sampling with the Sycamore quantum processor is in the middle between the perfect random quantum sampling and the classical uniform random sampling.

The difference among the Sycamore bit strings, the CUE bit strings, and the classical random bit strings is further illustrated using the random matrix theory of the random binary matrices. The collection $\{X_k\}$ of $n \times n$ matrices X_k of random bit strings can be regarded as a real Ginibre ensemble. It is well known that for random matrices with identically and independently distributed matrix elements with zero mean, the distribution of complex eigenvalues λ of random matrices follows the Girko circular law.[31,46] However, random matrices formed by random bit strings here have the matrix element $x_{ij} \in \{0, 1\}$, so the mean of a matrix X is not zero. If x_{ij} are sampled identically and independently from the Bernoulli distribution, the mean of X could be 1/2. We are interested in whether the mean of X generated by quantum random circuits is identical to 1/2 or not.

The distributions of the complex eigenvalues of random matrices $\left\{\frac{1}{\sqrt{n}}X^{(k)}\right\}$ with $k = 1, \ldots, 100$ are plotted in Figure 2. Most eigenvalues of both Sycamore and classical random matrices are distributed inside of the circle with radius 1/2, and some outliers with large real eigenvalues are located outside the circle. As shown in Figure 2, the positions of outliers with large real eigenvalues of Sycamore bit strings are different from that of the classical random bit strings. The radius 1/2 and the outliers can be explained as follows: The matrix X with nonzero mean can be transformed to Z with zero mean by

$$Z = 2X - J \tag{2}$$

where J is an all-one matrix. The ensemble of $n \times n$ real random square matrices (Z_k) with the matrix elements z_{ij} is sampled identically and independently from the Bernoulli distribution with zero mean and unit variance. The complex eigenvalues of $\frac{1}{\sqrt{n}}Z$ are distributed uniformly in the unit circle. So the radius of the circle of the eigenvalue distribution of X is

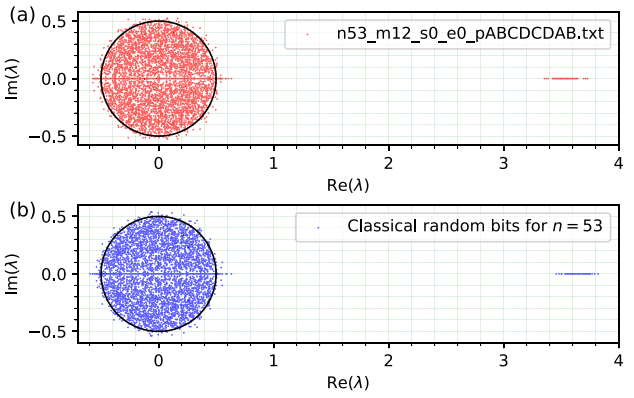

Figure 2. Distributions of complex eigenvalues λ of the $n \times n$ random bit matrices $\{X_k\}$ are shown for the Sycamore bit strings (a) and for the classical random bit strings (b) for $n = 53$. Only eigenvalues of 100 X_k samples are shown. The black circle is known as the Girko circle of the non-Hermitian Ginibre ensemble. The outliers far from the circle are the real eigenvalues located between 3 and 4.

1/2. The Saturn-ring effect along the real line[47,48] and the outliers shown in Figure 2 are due to the fact that X and J are noncommutative.

Let us slice the $M \times n$ random bit-string array D into $p \times n$ rectangular binary matrices X where $p > n$. Then, the collection of $n \times n$ symmetric matrices $W = \frac{1}{p}X^t \cdot X$ is called the Wishart ensemble. It is known that if the elements of X are sampled identically and independently from the normal distribution $\mathcal{N}(\mu, \sigma)$ with zero mean $\mu = 0$ and the variance σ^2, the distribution of real eigenvalues of W is given by the Marchenko–Pastur distribution[49]

$$\rho(\lambda) = \frac{1}{2\pi\gamma\sigma^2}\frac{\sqrt{(\lambda_+ - \lambda)(\lambda - \lambda_-)}}{\lambda} \tag{3}$$

where $\lambda_\pm = \sigma^2(1 \pm \sqrt{\gamma})^2$ are the upper and lower bounds and $\gamma = n/p$ is the rectangular ratio. Here we take $p = 2$. Figure 3 plots the Marchenko–Pastur distributions of the Sycamore bit strings and the classical random-bit strings for $n = 53$. As

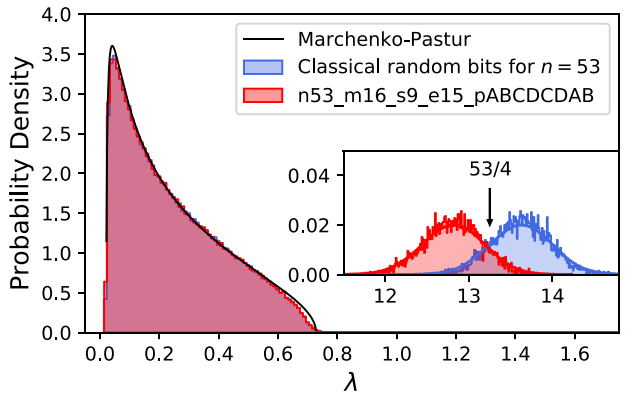

Figure 3. Marchenko–Pastur distribution of eigenvalues of Wishart ensembles for Sycamore bit strings and classical random bit strings. The inset shows the outlier of the Marchenko–Paster distribution that distinguishes the classical random bit strings and Sycamore bit strings.

https://doi.org/10.1021/acs.jpclett.2c02045
J. Phys. Chem. Lett. 2022, 13, 7469–7475

shown in Figure 3, the outliers outside the Marchenko−Pastur distribution distinguish the Sycamore bit strings from the classical random bit strings. With eq 2, W can be expressed as

$$W = \frac{1}{4p}(Z^t \cdot Z + Z^t \cdot J + J^t \cdot Z + J^t J) \tag{4}$$

Here the first term of eq 4 is to be written as $\frac{1}{p}\frac{Z^t}{2}\cdot\frac{Z}{2}$, so $\frac{Z}{2}$ has zero mean and variance $\sigma^2 = 1/4$ while the variance of X is $\sigma^2 = 1/2$. This gives the upper and lower bounds, $\lambda_+ = 0.728$ and $\lambda_- = 0.021$, respectively. The last term of eq 4 becomes $\frac{1}{4p}(J^t)_{n\times p}\cdot(J)_{p\times n} = 1/4(J)_{n\times n}$ where an all-one matrix J has the eigenvalues 0 and n. So the outliers are located around 53/4.

Up to now, we have shown that the Sycamore bit strings are different from CUE bit strings and classical random bit strings using heat maps and random matrix theory of random bit strings. The final question we would like to address is how different the Sycamore bit strings are from the CUE or classical random bit strings. In the quantum supremacy benchmark test for random quantum sampling,[7] the cross-entropy benchmark fidelity was used to measure how the experimental distribution is close to the ideal distribution. The disadvantage of the cross-entropy is that it is not symmetric and gives rise to zero or will diverge if there is no overlap between two distributions. To overcome these, we employ the Wasserstein distance of order 1, $W(p, q)$ between two discrete probability distributions, p_i and q_i

$$W(p, q) = \inf_{\pi_{ij}} \sum_{i,j} \pi_{i,j}|x_i - y_j| \tag{5}$$

where π_{ij} is a joint probability of x_i and y_j such that $\sum_i \pi_{i,j} = q_i$, $\sum_j \pi_{ij} = p_i$, and $\pi_{ij} \geq 0$. Given two samples, $\{x_1, x_2, ..., x_M\}$ and $\{y_1, y_2, ..., y_M\}$, $W(p, q)$ can be obtained directly without calculating the empirical distributions p and q. We use the python optimal transport library[50] for calculating the Wasserstein distance between two samples. Figure 4a presents the Wasserstein distances, normalized by N, between the Sycamore bit strings and the classical random bit strings as a function of n. For $n = 53$, the Sycamore data with the activation pattern with EFGH are closer to the classical random bits than those with ABCDCDAB. For $n = 12$, we calculate the Wasserstein distance among all pairs of the Sycamore bit strings, the CUE bit strings, and the classical random bit strings. The Sycamore data set for $n = 12$ qubits is available only for $m = 14$ cycles and is composed of the two subgroups: 10 files with 12 full qubits ranging from `n12-m14-s0-e0` to `n12-m14-s9-e0`, and the other 10 files with the 6th qubit elided ranging from `n12-m14-s0-e6` to `n12-m14-s9-e6`. These three data sets are located on the vertices of a triangle whose side lengths are given by Wasserstein distances (Classical) − (CUE), (CUE) − (Sycamore), and (Sycamore) − (Classical). So their relative locations in the two dimensions are displayed in Figure 4b. This shows that the Sycamore bit strings are farther from the CUE bit strings than the classical random bit sample. Also, all the Sycamore data except 2 data are fit to a straight line passing between the CUE and classical random bit samples. One can see that the Wasserstein distances of the Sycamore data from the CUE bit strings or the classical random bit strings are sensitive to random number seeds, $\{s0, ..., s9\}$.

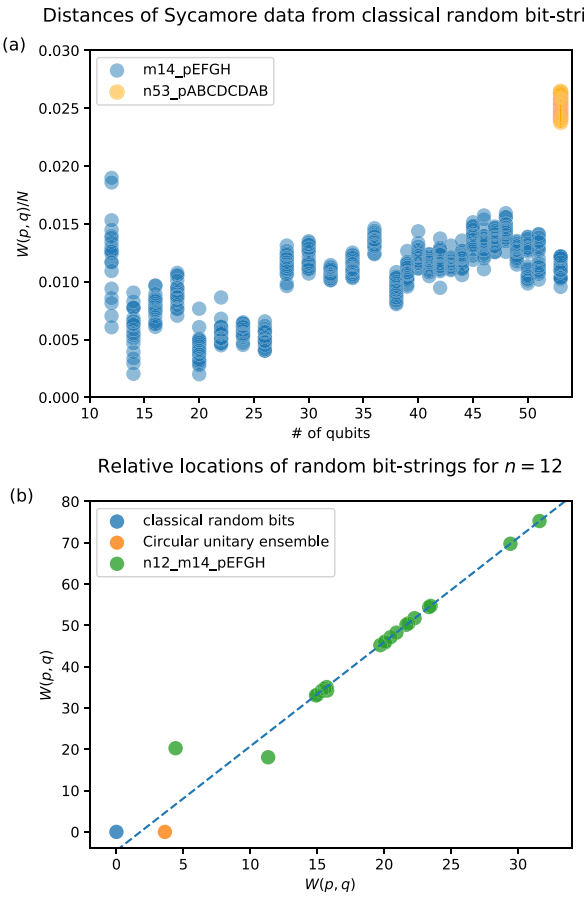

Figure 4. (a) Wasserstein distances between the Sycamore bit strings and the classical random bit strings, normalized by dividing by N, plotted as a function of the number of qubits, n. The blue and orange dots represent the activation patterns EFGH and ABCDCDAB, respectively. (b) For $n = 12$, all pairs of Wasserstein distances among the Sycamore bit strings, the CUE bit strings, and the classical random bit samples are calculated, and their relative locations are plotted. For each sample, $M = 500\,000$ is taken.

In conclusion, we analyzed the statistical properties of the Sycamore bit strings generated by random quantum circuits. It is found that the heat maps of the Sycamore data have stripe patterns at specific qubit sites. Also, the Sycamore bit strings contain more bit 0 than bit 1, which may be caused by readout errors. The Sycamore bit strings fail to pass the NIST random number tests. The random matrices of random bit strings distinguish the Sycamore data from the classical random bit strings. The calculation of the Wasserstein distance shows that the Sycamore bit strings are farther from the CUE bit strings than the classical random bit strings. The two activation patterns of the Sycamore quantum processors give rise to quite different results in the heat map of the bit strings and in the Wasserstein distances. Our findings imply that the random matrix analysis and the Wasserstein distance may be used as benchmark tools to measure the performance of intermediate scale quantum computers. The linear cross-entropy fidelity requires the quantum simulation on a classical computer to calculate the probability $p(x)$ of finding a bit string x. As the number of qubits increases, the quantum simulation becomes very difficult on a classical computer. So one faces the dilemma of how to verify the performance of quantum computers using the linear cross-entropy.[51] The calculation of the Wasserstein

https://doi.org/10.1021/acs.jpclett.2c02045
J. Phys. Chem. Lett. 2022, 13, 7469−7475

distance requires only two data sets of bit strings and does not need to estimate probability distributions from the two data sets. Classical random bit strings for one hundred qubits can be easily generated to calculate the Wasserstein distance between the classical random bit strings and the bit strings sampled from random quantum circuits.

As shown here, the statistical properties of bit strings sampled from random quantum circuits are affected by various errors. The same may be true of quantum simulation. For example, Sage et al. prepared condensates of photons on a 53 qubit quantum computer.[52] They reported that as the number of qubits increases, the deviations of the measured values of quantum simulation from the ideal values become large because of the accumulation of various errors. The characterization and mitigation of errors of intermediate-scale quantum computers is necessary to perform quantum simulation for large-scale molecules and realize quantum materials on quantum computers.

■ ASSOCIATED CONTENT

Supporting Information

The Supporting Information is available free of charge at https://pubs.acs.org/doi/10.1021/acs.jpclett.2c02045.

(i) Preparation of the data sets, (ii) additional heatmaps of bit strings sampled from Sycamore random quantum circuits, and (iii) NIST statistical tests for bit strings generated by random quantum circuits (PDF)

■ AUTHOR INFORMATION

Corresponding Author

Sabre Kais − *Department of Chemistry, Department of Physics and Astronomy, and Purdue Quantum Science and Engineering Institute, Purdue University, West Lafayette, Indiana 47907, United States;* orcid.org/0000-0003-0574-5346; Email: kais@purdue.edu

Author

Sangchul Oh − *Department of Chemistry, Department of Physics and Astronomy, and Purdue Quantum Science and Engineering Institute, Purdue University, West Lafayette, Indiana 47907, United States*

Complete contact information is available at: https://pubs.acs.org/10.1021/acs.jpclett.2c02045

Notes

The authors declare no competing financial interest.

■ ACKNOWLEDGMENTS

We thank Seth Lloyd, Scott Aaronson, and Sergio Boixo for reading and commenting on our draft manuscript. This material is based upon work supported by the U.S. Department of Energy, Office of Science, National Quantum Information Science Research Centers. We also acknowledge the National Science Foundation under Award Number 1955907.

■ REFERENCES

(1) Feynman, R. P. Simulating physics with computers. *International Journal of Theoretical Physics* **1982**, *21*, 467−488.

(2) Preskill, J. Quantum computing and the entanglement frontier. *arxiv* **2012**, 1203.5813; https://arxiv.org/abs/1203.5813.

(3) Harrow, A. W.; Montanaro, A. Quantum computational supremacy. *Nature* **2017**, *549*, 203−209.

(4) Shor, P. W. Polynomial-time algorithms for prime factorization and discrete logarithms on a quantum computer. *SIAM Journal on Computing* **1997**, *26*, 1484−1509.

(5) Harrow, A. W.; Hassidim, A.; Lloyd, S. Quantum algorithm for linear systems of equations. *Phys. Rev. Lett.* **2009**, *103*, 150502.

(6) Bouland, A.; Fefferman, B.; Nirkhe, C.; Vazirani, U. On the complexity and verification of quantum random circuit sampling. *Nat. Phys.* **2019**, *15*, 159−163.

(7) Arute, F.; Arya, K.; Babbush, R.; Bacon, D.; Bardin, J. C.; Barends, R.; Biswas, R.; Boixo, S.; Brandao, F. G. S. L.; Buell, D. A.; et al. Quantum supremacy using a programmable superconducting processor. *Nature* **2019**, *574*, 505−510.

(8) Wu, Y.; Bao, W.-S.; Cao, S.; Chen, F.; Chen, M.-C.; Chen, X.; Chung, T.-H.; Deng, H.; Du, Y.; Fan, D.; et al. Strong quantum computational advantage using a superconducting quantum processor. *Phys. Rev. Lett.* **2021**, *127*, 180501.

(9) Zhong, H.-S.; Wang, H.; Deng, Y.-H.; Chen, M.-C.; Peng, L.-C.; Luo, Y.-H.; Qin, J.; Wu, D.; Ding, X.; Hu, Y.; et al. Quantum computational advantage using photons. *Science* **2020**, *370*, 1460−1463.

(10) Troyansky, L.; Tishby, N. Permanent Uncertainty: On the quantum evaluation of the determinant and the permanent of a matrix. *Proc. PhysComp96* **1996**, 314−318.

(11) Aaronson, S.; Arkhipov, A. The computational complexity of linear optics. *Theory of Computing* **2013**, *9*, 143−252.

(12) Dyson, F. J. The threefold way. Algebraic structure of symmetry groups and ensembles in quantum mechanics. *Journal of Mathematical Physics* **1962**, *3*, 1199−1215.

(13) Pednault, E.; Gunnels, J. A.; Nannicini, G.; Horesh, L.; Wisnieff, R. Leveraging secondary storage to simulate deep 54-qubit Sycamore circuits. *arxiv* **2019**, 1910.09534; https://arxiv.org/abs/1910.09534.

(14) Huang, C.; Zhang, F.; Newman, M.; Cai, J.; Gao, X.; Tian, Z.; Wu, J.; Xu, H.; Yu, H.; Yuan, B. et al. Classical simulation of quantum supremacy circuits. *arxiv* **2020**, 2005.06787; https://arxiv.org/abs/2005.06787.

(15) Neill, C.; Roushan, P.; Kechedzhi, K.; Boixo, S.; Isakov, S. V.; Smelyanskiy, V.; Megrant, A.; Chiaro, B.; Dunsworth, A.; Arya, K.; et al. A blueprint for demonstrating quantum supremacy with superconducting qubits. *Science* **2018**, *360*, 195−199.

(16) Kuś, M.; Mostowski, J.; Haake, F. Universality of eigenvector statistics of kicked tops of different symmetries. *Journal of Physics A: Mathematical and General* **1988**, *21*, L1073−L1077.

(17) Haake, F.; Życzkowski, K. Random-matrix theory and eigenmodes of dynamical systems. *Phys. Rev. A* **1990**, *42*, 1013−1016.

(18) Blümel, R.; Smilansky, U. Random-matrix description of chaotic scattering: Semiclassical approach. *Phys. Rev. Lett.* **1990**, *64*, 241−244.

(19) Beenakker, C. W. J. Random-matrix theory of quantum transport. *Rev. Mod. Phys.* **1997**, *69*, 731−808.

(20) Haake, F.; Gnutzmann, S.; Kuś, M. *Quantum Signatures of Chaos*; Springer-Verlag: Berlin, 2010.

(21) Livan, G.; Novaes, M.; Vivo, P. *Introduction to Random Matrices − Theory and Practice*; Springer International Publishing, 2018.

(22) Emerson, J.; Weinstein, Y. S.; Saraceno, M.; Lloyd, S.; Cory, D. G. Pseudo-random unitary operators for quantum information processing. *Science* **2003**, *302*, 2098−2100.

(23) Emerson, J.; Alicki, R.; Życzkowski, K. Scalable noise estimation with random unitary operators. *Journal of Optics B: Quantum and Semiclassical Optics* **2005**, *7*, S347−S352.

(24) Knill, E.; Leibfried, D.; Reichle, R.; Britton, J.; Blakestad, R. B.; Jost, J. D.; Langer, C.; Ozeri, R.; Seidelin, S.; Wineland, D. J. Randomized benchmarking of quantum gates. *Phys. Rev. A* **2008**, *77*, 012307.

(25) Magesan, E.; Gambetta, J. M.; Emerson, J. Scalable and robust randomized benchmarking of quantum processes. *Phys. Rev. Lett.* **2011**, *106*, 180504.

(26) Hayden, P.; Preskill, J. Black holes as mirrors: quantum information in random subsystems. *Journal of High Energy Physics* **2007**, *2007*, 120−120.
(27) Nahum, A.; Vijay, S.; Haah, J. Operator spreading in random unitary circuits. *Phys. Rev. X* **2018**, *8*, 021014.
(28) Richter, J.; Pal, A. Simulating hydrodynamics on noisy intermediate-scale quantum devices with random circuits. *Phys. Rev. Lett.* **2021**, *126*, 230501.
(29) Martinis, J. M.; Boixo, S.; Neven, H.; Arute, F.; Arya, K.; Babbush, R.; Bacon, D.; Bardin, J. C.; Barends, R.; Biswas, R. Quantum supremacy using a programmable superconducting processor. *Nature* **2019**, 505.
(30) Mehta, M. L. *Random Matrices*; Pure and Applied Mathematics; Elsevier: Amsterdam, 2004; Vol. *142*.
(31) Tao, T.; Vu, V. Random matrices: Universality of local spectral statistics of non-Hermitian matrices. *Annals of Probability* **2015**, *43*, 782−874.
(32) Bassham, L.; Rukhin, A.; Soto, J.; Nechvatal, J.; Smid, M.; Leigh, S.; Levenson, M.; Vangel, M.; Heckert, N.; Banks, D. *A statistical test suite for random and pseudorandom number generators for cryptographic applications*. 2010; https://tsapps.nist.gov/publication/get_pdf.cfm?pub_id=906762.
(33) Villani, C. *Optimal Transport: Old and New*; Grundlehren der mathematischen Wissenschaften; Springer: Berlin, 2008.
(34) Hurwitz, A. *Mathematische Werke: Zweiter Band Zahlentheorie Algebra und Geometrie*; Springer: Basel, 1963; pp 546−564.
(35) Zyczkowski, K.; Kuś, M. Random unitary matrices. *Journal of Physics A: Mathematical and General* **1994**, *27*, 4235−4245.
(36) Mezzadri, F. How to generate random matrices from the classical compact groups. *Notices of the AMS* **2007**, *54*, 592−604.
(37) Boixo, S.; Isakov, S. V.; Smelyanskiy, V. N.; Babbush, R.; Ding, N.; Jiang, Z.; Bremner, M. J.; Martinis, J. M.; Neven, H. Characterizing quantum supremacy in near-term devices. *Nat. Phys.* **2018**, *14*, 595−600.
(38) Porter, C. E.; Thomas, R. G. Fluctuations of nuclear reaction widths. *Phys. Rev.* **1956**, *104*, 483−491.
(39) Brody, T. A.; Flores, J.; French, J. B.; Mello, P. A.; Pandey, A.; Wong, S. S. M. Random-matrix physics: spectrum and strength fluctuations. *Rev. Mod. Phys.* **1981**, *53*, 385−479.
(40) Aaronson, S.; Chen, L. Complexity-theoretic foundations of quantum supremacy experiments. 32nd Computational Complexity Conference (CCC 2017). Dagstuhl, Germany, 2017; pp 22:1−22:67.
(41) Aaronson, S.; Gunn, S. On the classical hardness of spoofing linear cross-entropy benchmarking. *arxiv* **2020**, 1910.12085; https://arxiv.org/abs/1910.12085.
(42) Markov, I. L.; Fatima, A.; Isakov, S. V.; Boixo, S. Quantum supremacy is both closer and farther than it appears. *arxiv* **2018**, 1807.10749; https://arxiv.org/abs/1807.10749.
(43) Chen, J.; Olver, S.; Nash, J.; Noack, A.; Rackauckas, C.; Micluta-Câmpeanu, S.; Squire, K.; Merberg, A.; Edelman, A.; Kelman, T. et al. JuliaMath/RandomMatrices.jl: v0.5.0. *Zenodo* **2019**; DOI: 10.5281/zenodo.3352200.
(44) Ang, S. K. Randomness_testsuite. 2019; https://github.com/stevenang/randomness_testsuite#readme.
(45) Oh, S.; Kais, S. Statistical analysis on random quantum sampling by Sycamore and Zuchongzhi quantum processors. *arxiv* **2022**, 2204.05875; https://arxiv.org/abs/2204.05875v1.
(46) Girko, V. L. Circular law. *Theory Probab. Appl.* **1985**, *29*, 694−706.
(47) Edelman, A.; Wang, Y. *Advances in Applied Mathematics, Modeling, and Computational Science*; Springer US, 2013; pp 91−116.
(48) Rider, B.; Sinclair, C. D. Extremal laws for the real Ginibre ensemble. *Annals of Applied Probability* **2014**, *24*, 1621.
(49) Marchenko, V. A.; Pastur, L. A. Distribution of eigenvalues for some sets of random matrices. *Mater. Sb. (N.S.)* **1967**, *72*, 507−526.
(50) Flamary, R.; Courty, N.; Gramfort, A.; Alaya, M. Z.; Boisbunon, A.; Chambon, S.; Chapel, L.; Corenflos, A.; Fatras, K.; Fournier, N.; et al. POT: Python optimal transport. *Journal of Machine Learning Research* **2021**, *22*, 1−8.
(51) Eisert, J.; Hangleiter, D.; Walk, N.; Roth, I.; Markham, D.; Parekh, R.; Chabaud, U.; Kashefi, E. Quantum certification and benchmarking. *Nature Reviews Physics* **2020**, *2*, 382−390.
(52) Sager, L. M.; Smart, S. E.; Mazziotti, D. A. Preparation of an exciton condensate of photons on a 53-qubit quantum computer. *Phys. Rev. Research* **2020**, *2*, 043205.

https://doi.org/10.1021/acs.jpclett.2c02045
J. Phys. Chem. Lett. 2022, 13, 7469−7475